⚡ Open Access

Iraqi Journal for Electrical and Electronic Engineering
Original Article

Bifurcation and Chaos from DTC Induction Motor Drive System

Ahmed Sadeq Hunaish*, Fadhil Rahma Tahir
Electrical Engineering Department, University of Basrah, Basrah, Iraq.

Correspondence
* Ahmed S. Hunaish
Electrical Engineering Department,
University of Basrah, Basrah, Iraq.
Email: *ahm782013@gmail.com*

Abstract
In this paper, three phase induction motor (IM) has been modelled in stationary reference frame and controlled by using direct torque control (DTC) method with constant V/F ratio. The obtained drive system consists of nine nonlinear first order differential equations. The numerical analysis is used to investigate the system behavior due to control parameter change. The integral gain of speed loop is used as bifurcation parameter to test the system dynamics. The simulation results show that the system has period-doubling route to chaos, period-1, period-2, period-4, and then the system gets chaotic oscillation. A specific value of the parameter range shows that the system has very strong randomness and a high degree of disturbance

KEYWORDS: *Bifurcation, chaos, direct torque control, induction motor.*

I. INTRODUCTION

Nowadays, the nonlinear behavior of systems is studied essential in nearly every domain of sciences and engineering. The nonlinear system can displays large diversity of behaviors produces the response solution hard to find in several states, even at what time numerical approaches are existing [1]. It is now a common belief that conception and employ the substantial dynamics, such as bifurcations and chaos, of nonlinear systems have an important influence on the modern technologies. Dynamic system behavior such as bifurcation and chaos are studied in many sections of engineering. Also chaos and its employment in machine drive systems have been excessively put out as published paper [2].

In electrical drive systems, there are many studies: in [3], [4] validation has been done by comparing with bifurcation diagram points in PSpice simulation and the obtained period-1, period-p and chaotic cases of the DC drive systems prototype. Reference [5] shows that the Hopf bifurcation and chaos have been appeared in permanent magnet synchronous machine (PMSM) dynamics, and then the theoretical analysis has been verified by the experimental result. Reference [6] proved the appearance of Hopf bifurcation and chaos in the synchronous reluctance motor drive system by using theoretical analysis and it is confirmed with computer simulations then validated experimentally. The bifurcation parameter is the compensator gain for the compensation of the raise of rotor resistance caused by prolonged operation. In the paper [7], Hopf bifurcation criterion for an IM drive system has been

obtained for different parameters such as stator resistance, rotor resistance and inertial constant. The work in [8] is concentrated onto analyze chaotic and bifurcation responses related to the scalar drives of the induction machine and a modified Poincare's map was demonstrated. Reference [9] used full order IM model to numerical analysis many types of bifurcations for proportional-integral-controlled indirect vector controlled IM, simulation and experiment results validation is used for saddle node and Hopf bifurcation has been offered. In [10], the PMSM dynamics is investigated to show the multi-stability and hidden-attractor in its dynamics.

All the above electric drive dynamic studies related to DC, PMSM, and induction motors drive systems. IM drives have key role in industrial applications, spatially the direct torque control (DTC). The dynamics behavior (bifurcations and chaos) of DTC drive system for IM are not mentioned in the previous literatures. This motivates us to investigate its dynamics.

In this paper, an IM with DTC driver is used to analyze the dynamics of the systems due to the variation of the PI torque loop parameters. Period-doubling route to chaos, period-1, period-2, period-4, period-5 and chaos are achieved by using computer simulation. The rest of paper is divided into: Section II, DTC IM system modelling contains the system scheme. Section III including the dynamical analysis of the system to find time response and phase portrait for a certain range of PI speed integral gain. Finally, conclusion is provided in section IV.

II. MODEL OF DTC IM DRIVE SYSTEM

DTC technique adopts vector states of output voltage based on the torque and stator flux magnitude errors by using space vector modulation (SVM) method without current loops [11]. In this section, the IM model and the overall IM drive model with DTC have been obtained.

The general stationary d–q model of a squirrel-cage induction motor can be stated according to [12], to have the following IM dynamic system:

$$\dot{\lambda}_{qs}^s = -R_s\left[\frac{L_r}{L_sL_r-L_m^2}\lambda_{qs}^s - \frac{L_m}{L_sL_r-L_m^2}\lambda_{qr}^{s\prime}\right] + v_{qs}^s \qquad (1)$$

$$\dot{\lambda}_{ds}^s = -R_s\left[\frac{L_r}{L_sL_r-L_m^2}\lambda_{ds}^s - \frac{L_m}{L_sL_r-L_m^2}\lambda_{dr}^{s\prime}\right] + v_{ds}^s \qquad (2)$$

$$\dot{\lambda}_{qr}^{s\prime} = -R_r'\left[-\frac{L_m}{L_sL_r-L_m^2}\lambda_{qs}^s + \frac{L_s}{L_sL_r-L_m^2}\lambda_{qr}^{s\prime}\right] + \omega_r \qquad (3)$$

$$\dot{\lambda}_{dr}^{s\prime} = -R_r'\left[-\frac{L_m}{L_sL_r-L_m^2}\lambda_{ds}^s + \frac{L_s}{L_sL_r-L_m^2}\lambda_{dr}^{s\prime}\right] - \omega_r\,\lambda_{qr}^{s\prime} \qquad (4)$$

$$\dot{\omega}_r = \frac{P}{2}\frac{1}{j}\left(\frac{3P}{4}\frac{L_m}{L_sL_r-L_m^2}\left(\lambda_{qs}^s\lambda_{dr}^{s\prime} - \lambda_{ds}^s\lambda_{qr}^{s\prime}\right) - T_l \right) \qquad (5)$$

where: λ_{qs}^s, λ_{ds}^s, $\lambda_{qr}^{s\prime}$, and $\lambda_{dr}^{s\prime}$ are the stator and rotor fluxes in quadrature and direct axis referred to stator, respectively, and ω_r is the rotor speed. The system parameters are defined in Table I.

The DTC scheme with constant voltage to frequency ratio is shown in Fig. 1. The controller outputs are the magnitude and angle of the voltage of the motor stator.
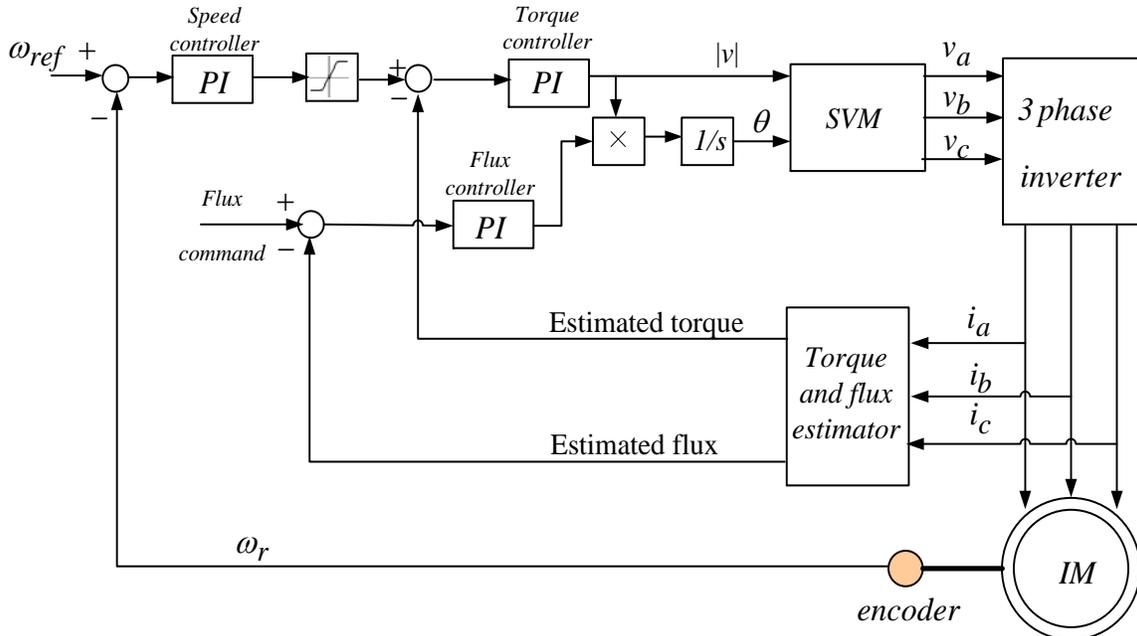
TABLE I
System Parameters Definition

Parameter	Definition	Parameter	Definition
R_s	Stator resistance	P	Number of poles
L_s	Stator inductance	T_l	Load torque
R_r'	Rotor resistance	k_{ps} and k_{is}	Speed PI gains
L_r'	Rotor inductance	k_{pT} and k_{iT}	Torque PI gains
L_m	Mutual inductance	k_{pf} and k_{if}	Flux PI gains
J	Rotor inertia	λ_s^*	The stator reference flux

According to these outputs, the space vector modulation (SVM) is designed and applied to the three phase inverter which supplies the three phase induction motor.

By defining nine state variables, $x_1 = \lambda_{qs}^s$, $x_2 = \lambda_{ds}^s$, ,$x_3 = \lambda_{qr}^{s\prime}$, $x_4 = \lambda_{dr}^{s\prime}$, $x_5 = \omega_r$, $x_6 = (k_{ps} + k_{is}\int dt)(\omega_{ref} - \omega_r)$, $x_7 = (k_{pT} + k_{iT}\int dt)(T_e^* - \widehat{T}_e)$, $x_8 = (k_{pf} + k_{if}\int dt)(\lambda_s^* - \widehat{\lambda}_S)$, and $x_9 = \theta$, the DTC model can be given as following:

$$\dot{x}_1 = -R_s[c_1x_1 - c_2x_3] + v_{qs}^s \qquad (6)$$

$$\dot{x}_2 = -R_s[c_1x_2 - c_2x_4] + v_{ds}^s \qquad (7)$$

Fig. 1: DTC drive system scheme.

$$\dot{x}_3 = R'_r[c_2 x_1 - c_3 x_3] + x_4 x_5 \tag{8}$$

$$\dot{x}_4 = R'_r[c_2 x_2 - c_3 x_4] - x_3 x_5 \tag{9}$$

$$\dot{x}_5 = \dot{x}_5 = \frac{P}{2}\frac{1}{J}(\frac{3P}{4}c_2(x_1 x_4 - x_2 x_3) - T_l) \tag{10}$$

$$\dot{x}_6 = k_{ps}(\dot{\omega}_r^* - \frac{P}{2J}(\frac{3P}{4}c_2(x_1 x_4 - x_2 x_3) - T_l) + \\ k_{is}(\omega_r^* - x_5) \tag{11}$$

$$\dot{x}_7 = k_{pT}\left(\dot{x}_6 - \frac{3P}{4}c_2(x_4\dot{x}_1 - x_3\dot{x}_2 - x_2\dot{x}_3 + \\ x_1\dot{x}_4)\right) + k_{iT}(x_6 - \frac{3P}{4}c_2(x_1 x_4 - x_2 x_3)) \tag{12}$$

$$\dot{x}_8 = k_{if}\left(\lambda_s^* - \sqrt{x_1^2 + x_2^2}\right) - k_{pf}\frac{(x_1+x_2)}{(x_1^2+x_2^2)^{1/2}} \tag{13}$$

$$\dot{x}_9 = x_7 x_8 \tag{14}$$

where $c_1 = \frac{L_r}{L_s L_r - L_m^2}$, $c_2 = \frac{L_m}{L_s L_r - L_m^2}$, and $c_3 = \frac{L_s}{L_s L_r - L_m^2}$

III.   DYNAMICAL ANALYSIS

The nonlinear dynamical system "(6)" through "(14)", gives the bifurcation occurs with the variation of the system parameter. In fact, numerical analysis is helpful for higher order dynamic systems where mathematical analysis perhaps is not efficient. The familiar tools that are used to investigate the system dynamics are the bifurcation diagram and Lyapunov exponent spectrum.

The motor parameters are listed in Table II [13]. The controller parameters are set to: $k_{pf} = k_{if} = 0.01$, $k_{pT} = k_{iT} = 1$, $k_{ps} = 0.001$. While k_{is} is selected as the bifurcation parameter.

The reference speed (ω_{ref}) is set to 314 rad/sec at no load and the reference flux is determined approximately from magnitude of motor voltage ($|v|$) and the voltage frequency (f) as following [14]:

$$\lambda_s^* = \frac{|v|}{2\pi f} \tag{15}$$

From Fig.2 (a), the phase portrait of speed (x_5) and PI controller output of the speed of the motor (x_6), one can note that for $k_{is}=90$, the system operates normally where the motor speed tracks the command speed (stable fixed point). Fig.2 (b) represents the time response of the motor speed.

A stable periodic solution is occurred (period-1) at $k_{is}=91.4$, Fig. 2 (c) and (d) illustrates the phase portrait of x_6 and x_5 and the time response of the motor speed with $k_{is}=100$, respectively.

Period doubling is appeared as period-2 at $k_{is}=105.4$ to $k_{is}=108.3$, a sample has been plotted in Fig. 2 (e) and (f) with $k_{is}=106$, it is clear that the speed waveform has two different amplitudes and frequencies.

Period-4 is noted at $k_{is}= 108.4$. Fig. 2 (g) and (h) represent the phase plane of speed and speed difference PI

output and the time series of the motor speed, respectively with $k_{is}=108.8$.

TABLE II
IM Parameters

Parameter	Value	Parameter	Value
Nominal voltage (V)	220	Stator inductance (mH)	43.9
Supply frequency (Hz)	50	Rotor resistance (Ω)	3
Rated speed (rpm)	1430	Rotor inductance (mH)	43.9
Number of poles	4	Mutual inductance (mH)	278
Stator resistance (Ω)	3.3	Rotor inertia (kgm²)	0.00665

The period-4 above was the route to no periodic solution (chaos), the chaos speed is appeared at $k_{is}=109$. The phase portrait and the time response which represent the chaos case are shown in Fig. 2 (i) and (j), respectively. In Fig. 2 (j) with $k_{is}=250$, the motor speed oscillates in chaotic manner with very large number of waves which differ in amplitude and oscillation size.

IV.   CONCLUSION

The three phase IM has been modelled in stationary reference frame and controlled by using DTC method with constant V/F ratio. The numerical analysis is used to investigate the system behavior due to control parameter change. The integral gain variation of speed loop is used to test the system dynamics. The simulation results show that the system has been bifurcated into period-1, -2, -4, and then the system to be chaotic oscillation, the time response and phase portrait figures assigned these situations. Fig. 2 (j) reflects very strong chaotic oscillation in the motor speed.

CONFLICT OF INTEREST

The authors have no conflict of relevant interest to this article.

REFERENCES

[1] S. Rugonyi and K. J. Bathe, "An evaluation of the Lyapunov characteristics exponent of chaotic continuous systems," Int. J. Numer. Methods Eng., vol. 56, no. 1, pp. 145–163, 2003.

[2] K. T. Chua and Zheng Wang, Chaos in Electrical Drive Systems: Analysis, Control and Application, ingapore: John Wiley & Sons (Asia), 2011.

[3] J. K. H. Chau, K. T., Chen, J. H., Chan , C. C., & Pong, "Chaotic behavior in a simple DC drive," in Proceedings of Second International Conference on Power Electronics and Drive Systems, pp. 523–528, 1997.

[4] J. H. Chen, K. T. Chau, and C. C. Chan, "Analysis of chaos in current-mode-controlled DC drive systems," vol. 47, no. 1, pp. 67–76, 2000.
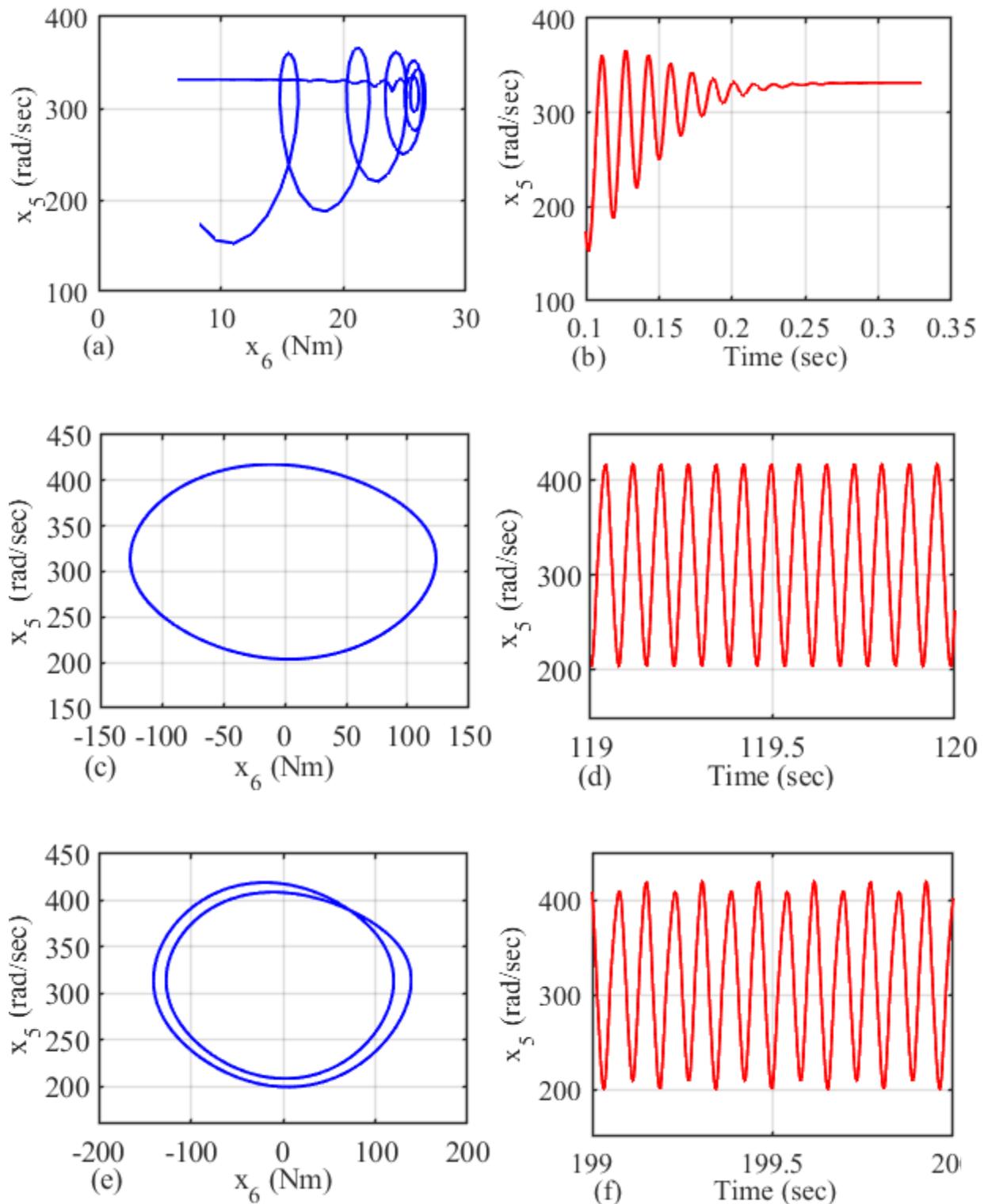
Fig. 2: Projection onto (x_6, x_5) (left column) and time response of x_5 (right column) : (a) Fixed point: phase portrait and (b) time response at k_{is} =91; (c) Period-1: phase portrait and (d) time response at k_{is}=100; (e) Period-2: phase portrait and (f) time response at k_{is}=106; (g) Period-4: phase portrait and (h) time response at k_{is}= 108.8; (i) Chaos attractor: phase portrait and (j) time response at k_{is}=250.
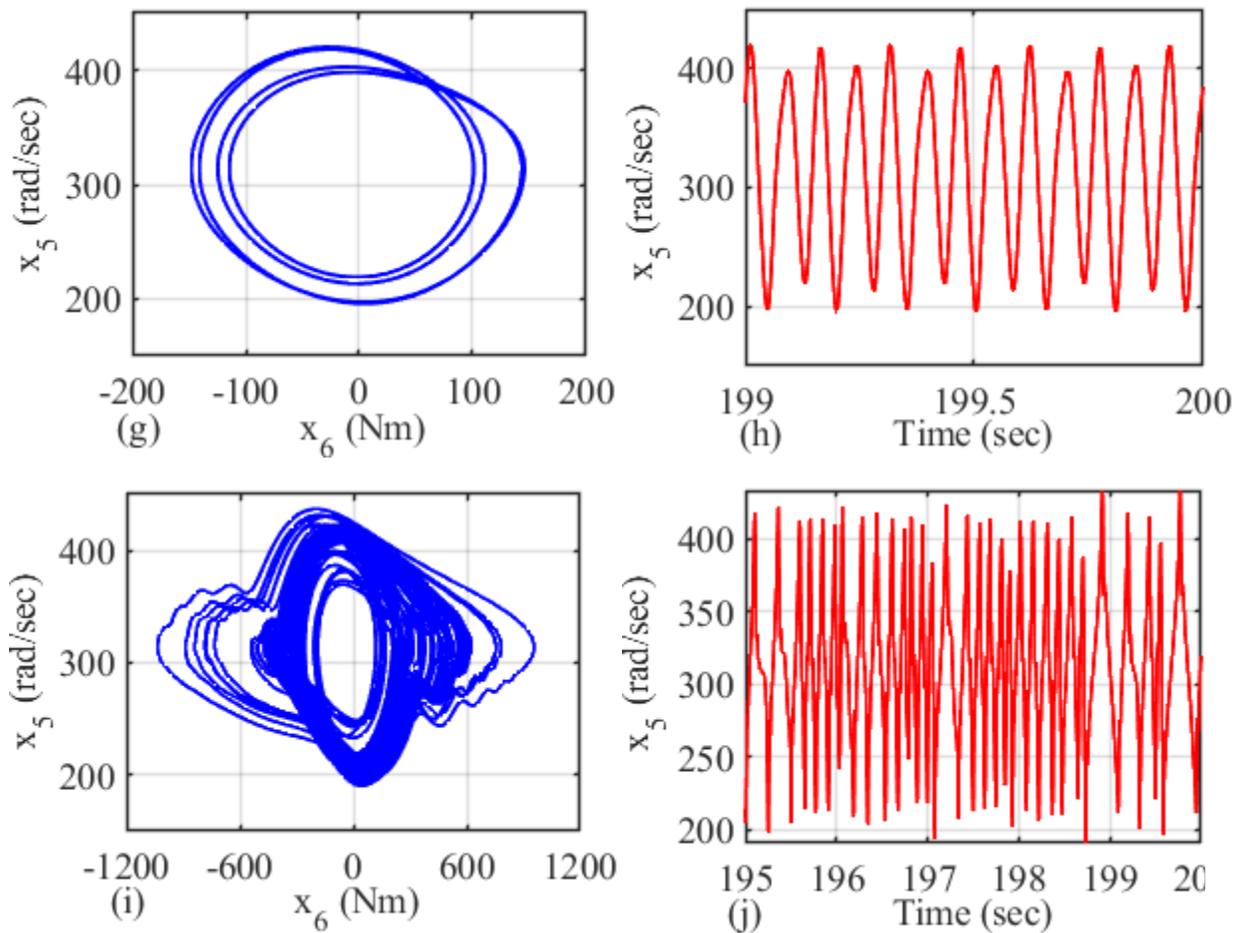
Fig. 2: (continued)

[5] K. T. Gao, Y and Chau, "Design of permanent magnets to avoid chaos in PM synchronous machines," IEEE Trans. Magn., vol. 39, no. 5, pp. 2995–2997, 2003.

[6] Y. Gao and K. T. Chua, "Hopf bifurcation and chaos in synchronous reluctance motor drives," IEEE Trans. ENERGY Convers., vol. 19, no. 2, pp. 296–302, 2004.

[7] H. Li and X. Li, "Hopf bifurcation criterion and control of the induction motor drive system," The 3 IEEE Conference on Industrial Electronics and Application, 3-5 June, 2008.

[8] R. A. Sangrody, J. Nazarzadeh, and K. Y. Nikravesh, "Bifurcation and Lyapunov's exponents characteristics of electrical scalar drive systems," IET Power Electron., vol. 5, no. 7, pp. 1236–1244, 2012.

[9] J. K. Jain, S. Ghosh, and S. Maity, "A numerical bifurcation analysis of indirect vector-controlled induction motor," IEEE Trans. Control Syst. Technol., vol. 26, no. 1, pp. 282-290, 2018.

[10] J. P. Singh, B. K. Roy, and N. V. Kuznetsov, "Multistability and hidden attractors in the dynamics of permanent magnet synchronous motor," Int. J. Bifurc. Chaos, vol. 29, no. 4, pp. 1–17, 2019.

[11] B. K. Bose, Modern Power Electronics and AC Drives, Prentice Hall PTR, USA, 2001.

[12] C.-M. Ong, Dynamic Simulation of Electric Machinery Using Matlab /Simulink, Prentice Hall PTR, 1998.

[13] Z. Zhang, K. T. Chau, and Z. Wang, "Chaotic speed synchronization control of multiple induction motors using stator flux regulation," IEEE Trans. Magn., vol. 48, no. 11, pp. 4487–4490, 2012.

[14] N. Pimkumwong and M. S. Wang, "Full-order observer for direct torque control of induction motor based on constant V/F control technique," ISA Trans., vol. 73, pp. 189–200, 2018.